

Symmetry-Breaking in Multi-Agent Navigation: Winding Number-Aware MPC with a Learned Topological Strategy

Tomoki Nakao^{*,1}, Kazumi Kasaura^{*,2}, and Tadashi Kozuno²

¹Graduate School of Informatics, Kyoto University, Kyoto, Japan. This work was done while he was a research intern at OMRON SINIC X Corporation.

nakao.tomoki.54e@st.kyoto-u.ac.jp

²OMRON SINIC X Corporation, 5-24-5, Hongo, Bunkyo-ku, Tokyo, Japan.

{kazumi.kasaura, tadashi.kozuno}@sinicx.com

^{*}Equal contribution.

Abstract

We address the fundamental challenge of resolving symmetry-induced deadlocks in distributed multi-agent navigation by proposing a new hierarchical navigation method. When multiple agents interact, it is inherently difficult for them to autonomously break the symmetry of deciding how to pass each other. To tackle this problem, we introduce an approach that quantifies cooperative symmetry-breaking strategies using a topological invariant called the winding number, and learns the strategies themselves through reinforcement learning. Our method features a hierarchical policy consisting of a learning-based Planner, which plans topological cooperative strategies, and a model-based Controller, which executes them. Through reinforcement learning, the Planner learns to produce two types of parameters for the Controller: one is the topological cooperative strategy represented by winding numbers, and the other is a set of dynamic weights that determine which agent interaction to prioritize in dense scenarios where multiple agents cross simultaneously. The Controller then generates collision-free and efficient motions based on the strategy and weights provided by the Planner. This hierarchical structure combines the flexible decision-making ability of learning-based methods with the reliability of model-based approaches. Simulation and real-world robot ex-

periments demonstrate that our method outperforms existing baselines, particularly in dense environments, by efficiently avoiding collisions and deadlocks while achieving superior navigation performance. The code for the experiments is available at <https://github.com/omron-sinicx/WNumMPC>.

1 Introduction

The multi-agent navigation problem considers multiple agents moving in a shared space to reach their respective goals while avoiding collisions. This problem is central to many robotics applications such as warehouse automation and traffic management, and has been studied from various perspectives. A straightforward approach is centralized navigation; however, it requires inter-agent communication and scales poorly computationally for large systems [1, 2], making deployment in real-world settings challenging. In contrast, distributed navigation does not require explicit communication and is scalable with respect to the number of agents; thus, it has received significant attention [3–5]. In distributed settings, since others’ intentions (e.g., goals) are unobservable, agents must plan cooperatively, going beyond purely local collision avoidance.

A key challenge arises from *symmetry* among agents in

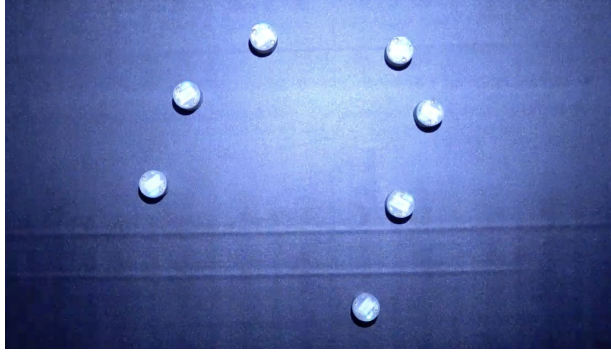


Figure 1: Seven small two-wheeled robots (“maru” [9]) moving on a tabletop. By cooperatively breaking positional symmetry, the system achieves efficient navigation.

the absence of explicit communication or priority. For example, when two agents approach each other, they may fail to decide on a passing side and become stuck [6]. Such symmetry-induced deadlocks are a major obstacle for distributed navigation; the system needs to recognize interactions and *break symmetry* cooperatively. Incorporating the *topological* relation between trajectories is effective for this purpose [7, 8]. In particular, the winding number provides a topological invariant that abstracts the essence of “passing”, enabling a quantitative description of how trajectories wind around each other.

In this work, we address symmetry-breaking for distributed navigation by proposing a winding-number-aware navigation algorithm. Our method adopts a hierarchical policy with a learning-based Planner that determines global cooperative strategy and a model-based Controller that executes local collision avoidance. The Planner learns both a topological cooperative strategy represented as a winding number and dynamic weights indicating which agents to prioritize for coordination. The Controller then executes local control to follow the plan.

Contributions

In this work, we address the fundamental challenge of deadlocks caused by positional symmetry in distributed navigation, and propose a new hierarchical navigation method that learns cooperative strategies for symmetry

breaking via reinforcement learning. The framework of our proposed method is illustrated in Fig. 2. The contributions of this paper are as follows:

- **A hierarchical framework that unifies strategy planning and reliable execution:** We propose a new hierarchical architecture that separates the planning and execution of cooperative strategies, enabling reliable real-world execution of strategies learned through reinforcement learning. This division of roles allows us to combine the flexibility of RL-based strategy acquisition with the reliability of model-based control.
- **Learning topological cooperative strategies for symmetry breaking:** We introduce a novel approach that directly learns winding numbers as cooperative strategies involving symmetry breaking. By learning target winding numbers as continuous values, the Planner can plan appropriate cooperative strategies even in situations where rule-based methods fail.
- **Dynamic weighting for prioritizing multi-agent cooperation:** In dense environments where multiple agents cross simultaneously, the Planner learns dynamic weights that correspond to the importance of cooperation with each agent. By incorporating these weights into the Controller’s cost function, interactions can be considered only when necessary.

We validate the effectiveness of our method through extensive simulation and real-world experiments with tabletop robots named *maru* (Fig. 1). By comparing against established baselines, we quantitatively demonstrate the advantages of learning topological cooperative strategies and employing a hierarchical architecture.

2 Related Work

Distributed multi-agent navigation is a challenging problem and an actively studied area. Reactive methods such as [10–12] achieve collision avoidance by considering one-step interactions based on geometric or physical relations. These approaches offer excellent computational efficiency; however, since they do not account for the temporal evolution of the states of surrounding agents, they

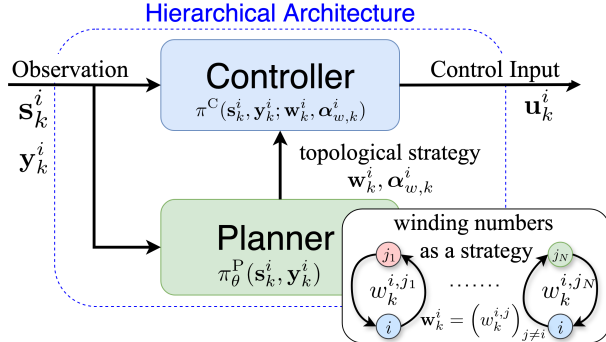


Figure 2: The proposed hierarchical architecture for cooperative symmetry breaking. The learning-based Planner generates a high-level topological strategy to break symmetry, which the model-based Controller then executes reliably.

are known to result in short-sighted behaviors [3]. To address this limitation, trajectory-based methods have been proposed that plan navigation based on long-horizon predictions. For example, [13] estimates the local goals of surrounding agents using constant-velocity assumptions and performs model-based planning over a long horizon. However, these approaches rely entirely on hand-crafted rules or cost functions, which limits their ability to achieve cooperative behaviors and generalize to dense environments with complex interactions. In particular, when the spatial relations among agents are symmetric, agents may give way to each other, leading to deadlocks. To overcome the limitations in cooperativeness and generalization, many learning-based methods have been explored. Approaches such as [3–5] learn policies online that account for inter-agent interactions to achieve collision avoidance. CADRL and its variants [3–5] employ reinforcement learning to refine policies after pretraining with trajectories from ORCA [12]. However, this framework inherits the limitations of ORCA [14].

A fundamental difficulty common to the above methods lies in cooperative decision-making that requires breaking symmetry. A promising direction is to focus on the topological relations among trajectories. In particular, [7, 8] propose to quantify cooperative strategies that involve symmetry breaking using the *winding number* [15], a topological pairwise feature. Specifically, [7] applies discrete

winding numbers estimated between agents to distributed navigation, while [8] incorporates winding numbers into the cost function of robot controllers, selecting control inputs to maximize the absolute value of predicted winding numbers and thereby achieving efficient crowd navigation.

Despite these contributions, challenges remain in how topological cooperative strategies are handled. First, both [7, 8] rely on hand-crafted cost functions or estimation models to select winding numbers, limiting flexibility in complex situations beyond what the designer anticipated. Moreover, treating winding numbers as discrete values reduces the expressiveness of cooperative strategies. Finally, [7] suffers from computational complexity $O(2^{n(n-1)/2})$ with respect to the number n of agents, which hampers scalability.

Other topological concepts have also been explored for multi-agent navigation. For instance, some works have utilized braid theory [16, 17] to represent agent interactions, which can capture finer topological characteristics for systems with more than two agents. However, we choose to build upon the winding number for two key reasons. First, its ability to be treated as a continuous quantity makes it naturally applicable to scenarios where other agents' goals are unknown and facilitates its integration into an MPC cost function. Second, prior works [7, 8] have already demonstrated its practical effectiveness. Another hierarchical approach [18] computes topological features by enumerating crossings with edges in a graph connecting other agents. This method, however, is less suitable for the dense crossing scenarios we consider, as the graph's topology can change rapidly and unpredictably.

Finally, we clarify the scope of our work. The winding number can also be used for representation of ways to avoid collision with stable obstacles [19]. While we focus on multi-agent navigation in an obstacle-free environment in our experiment, our framework is applicable to collision avoidance strategies with stable obstacles. Furthermore, whereas several previous works using topological notions have considered human-robot interaction [8, 16–18, 20], this paper concentrates on navigation among multiple robots that share a common policy.

3 Preliminaries

In this section, we formulate the navigation problem for a decentralized multi-agent system, and define the winding number [15] to quantify the topological cooperative strategy governing how agents pass one another.

3.1 Problem Formulation

Following [3–5], distributed multi-agent navigation is modeled as a partially observable decision-making problem. Let $N \in \mathbb{Z}_+$ be the number of agents and $\mathcal{A} := \{1, \dots, N\}$ be the set of agent indexes. The state of agent $i \in \mathcal{A}$ at time $k \in \mathbb{Z}_{\geq 0}$ is denoted by $\mathbf{s}_k^i := [\mathbf{s}_k^{i,o\top}, \mathbf{s}_k^{i,h\top}]^\top$, where $\mathbf{s}^o := [p_x, p_y, v_x, v_y, r] \in \mathbb{R}^5$ denotes observable quantities (position $\mathbf{p} = [p_x, p_y]^\top$, velocity $\mathbf{v} = [v_x, v_y]^\top$, radius r) and $\mathbf{s}^h := [p_{gx}, p_{gy}, \theta]^\top \in \mathbb{R}^3$ denotes hidden quantities (goal position $\mathbf{p}_{\text{goal}} = [p_{gx}, p_{gy}]$ and heading θ). Let $\mathcal{U} \subset \mathbb{R}^2$ be the action space and $\mathbf{u}_k^i \in \mathcal{U}$ the control input of agent i at time k . All agents share the same deterministic dynamics $f: \mathbb{R}^9 \times \mathbb{R}^2 \rightarrow \mathbb{R}^9$:

$$\mathbf{s}_{k+1}^i = f(\mathbf{s}_k^i, \mathbf{u}_k^i), \quad (\mathbf{s}_0^i: \text{given}, \forall i \in \mathcal{A}).$$

Each agent uses a shared policy π such that $\mathbf{u}_k^i \sim \pi(\mathbf{s}_k^i, \mathbf{y}_k^i)$, where $\mathbf{y}_k^i := \{\mathbf{s}_k^{j,o} \mid j \in \mathcal{A} \setminus \{i\}\}$ denotes the observable states of others. The optimal control problem for a decentralized multi-agent system is formulated as follows.

Problem 1 (Multi-Agent Navigation Problem) *Given initial states $\{\mathbf{s}_{i,0}\}_{i \in \mathcal{A}}$, find a memoryless policy π that minimizes the expected time $k_g \in \mathbb{N}$ for all agents to reach their goals:*

$$\begin{aligned} & \arg \min_{\pi} \mathbb{E}_{\pi} [k_g \mid \{\mathbf{s}_{i,0}\}_{i \in \mathcal{A}}] \\ \text{s.t. } & \|\mathbf{p}_k^i - \mathbf{p}_k^j\|_2 > r_i + r_j \quad (\forall i, j \in \mathcal{A}, i \neq j), \\ & \mathbf{p}_{k_g}^i = \mathbf{p}_g^i \quad (\forall i \in \mathcal{A}), \\ & \mathbf{s}_{k+1}^i = f(\mathbf{s}_k^i, \mathbf{u}_k^i), \quad \mathbf{u}_k^i \sim \pi(\mathbf{s}_k^i, \mathbf{y}_k^i) \quad (\forall i \in \mathcal{A}). \end{aligned}$$

△

The objective of this problem is to minimize the time required for all agents to reach their respective goals.

3.2 Winding Number

Symmetry-induced deadlocks frequently occur in distributed navigation when agents occupy symmetric configurations. Breaking such symmetry requires behavior driven by a *topological* passing strategy. We adopt the winding number [15] as a quantitative invariant for such strategy. Following [7, 8], for two trajectories on the plane we define:

Definition 1 (Winding Number) *Let $\theta_k^{i,j}$ be the bearing of agent j from agent i at time k . For the pair of observable trajectories $(\mathbf{s}_{k:l}^{i,o}, \mathbf{s}_{k:l}^{j,o})$ from time k to l , the winding number w is*

$$w(\mathbf{s}_{k:l}^{i,o}, \mathbf{s}_{k:l}^{j,o}) := \frac{1}{2\pi} \sum_{\bar{k}=k}^{l-1} \Delta\theta_{\bar{k}}^{i,j},$$

where $\Delta\theta_{\bar{k}}^{i,j} \in (-\pi, \pi]$ is the signed angle between $\theta_{\bar{k}}^{i,j}$ and $\theta_{\bar{k}+1}^{i,j}$. □

The sign of w encodes the passing side, and its magnitude reflects progress toward passing. Selecting an appropriate target w thus corresponds to choosing a concrete strategy for symmetry breaking. By acting to make the predicted winding number match the target, an agent achieves the planned cooperative behavior. Although w is pairwise, prior work has shown it remains informative in scenarios with multiple simultaneous crossings [7, 8]. In our method, the Planner learns target values $w^{i,j}$ to enable cooperative symmetry breaking.

4 Proposed Method

Choosing a topology (via the winding number) breaks symmetry and avoids deadlocks, but selecting it by hand-crafted rules is difficult. We therefore propose a Planner π_{θ}^P that *learns* both topological cooperative strategy and its dynamic weights. Combined with a model-based Controller π^C in a hierarchy, our method marries the flexibility of learning with the reliability of model-based control to address Problem 1.

4.1 Winding Number Planner

The learning-based Planner π_{θ}^P maps observations to a topological cooperative plan that breaks symmetry. Con-

cretely, it outputs target winding numbers relative to other agents. In addition, it determines the dynamic cost weights to indicate which interactions to prioritize, which enables flexible navigation even in dense environments.

Formally, the Planner is defined as follows:

$$\mathbf{w}_k^i, \boldsymbol{\alpha}_{w,k}^i \sim \pi_\theta^P(\mathbf{s}_k^i, \mathbf{y}_k^i),$$

$$\mathbf{w}_k^i := \left(w_k^{i,j} \right)_{j \neq i}, \quad \boldsymbol{\alpha}_{w,k}^i := \left(\alpha_{w,k}^{i,j} \right)_{j \neq i}.$$

Here $w_k^{i,j} \in \mathbb{R}$ is the target winding number for agent i and j from time k to the end of the prediction horizon, and $\alpha_{w,k}^{i,j}$ is the weight used in the cost terms of (1)–(2). The network parameters for Planner are denoted by θ . Inputs $(\mathbf{s}_k^i, \mathbf{y}_k^i)$ are represented in a rotation-invariant local frame, following [3–5], to avoid geometric redundancy.

We train π_θ^P with PPO [21]. All agents share parameters θ , collect rollouts into a common replay buffer, and optimize the shared planner. The objective is

$$J(\pi) := \mathbb{E}_\pi \left[\sum_{k=0}^{K_{\max}} \gamma^k r(\mathbf{s}_k, \mathbf{u}_k) \right],$$

with reward shaped as in [3–5]:

$$r(\mathbf{s}_k, \mathbf{u}_k) := \begin{cases} -1 & (d_{\min} < 0) \\ 1.5 \cdot (d_{\min} - 0.25)/2 & (d_{\min} < 0.25) \\ 1 & (\mathbf{p} = \mathbf{p}_g) \\ 0 & (\text{otherwise}), \end{cases}$$

where d_{\min} is the distance to the nearest other agent, \mathbf{p} the current position, and \mathbf{p}_g the goal. The discount factor is γ . While the reward is calculated independently for each agent, episode termination is determined from the states of all agents. Episodes terminate for all agents upon any collision to encourage cooperative avoidance. As in [3–5], we decay rewards quickly by setting $\gamma = 0.95 < 1$ to encourage efficient navigation.

4.2 Winding Number-aware Controller

The model-based Controller π^C produces concrete control inputs \mathbf{u}_k^i that realize the planned topology, given the target winding numbers \mathbf{w}_k^i and weights $\boldsymbol{\alpha}_{w,k}^i$ of winding number costs. Formally,

$$\mathbf{u}_k^i = \pi^C(\mathbf{s}_k^i, \mathbf{y}_k^i; \mathbf{w}_k^i, \boldsymbol{\alpha}_{w,k}^i).$$

It is implemented as MPC [22]. At each step, we solve

$$\begin{aligned} \arg \min_{\bar{\mathbf{u}}_{0:K}} \mathcal{J}(\bar{\mathbf{s}}_{0:K}^i, \bar{\mathbf{y}}_{0:K}^i; \mathbf{w}_k^i, \boldsymbol{\alpha}_{w,k}^i) \\ \text{s.t. } \bar{\mathbf{s}}_{k+1}^i = f(\bar{\mathbf{s}}_k^i, \bar{\mathbf{u}}_k^i), \quad \bar{\mathbf{s}}_0^i = \mathbf{s}_k^i, \quad \bar{\mathbf{y}}_0^i = \mathbf{y}_k^i, \end{aligned}$$

and apply the initial action $\mathbf{u}_0^{*,i}$ of the optimal sequence $\mathbf{u}_{0:K}^{*,i}$ as \mathbf{u}_k^i . Here, $K \in \mathbb{N}$ is the prediction horizon, and future trajectories $\bar{\mathbf{y}}_k^i$ of other agents are approximated by constant-velocity extrapolation. The cost is

$$\begin{aligned} \mathcal{J}(\bar{\mathbf{s}}_{0:K}^i, \bar{\mathbf{y}}_{0:K}^i; \mathbf{w}_k^i, \boldsymbol{\alpha}_{w,k}^i) &:= \alpha_g \mathcal{J}_g(\bar{\mathbf{s}}_{0:K}^i) \\ &+ \alpha_o \mathcal{J}_o(\bar{\mathbf{s}}_{0:K}^i, \bar{\mathbf{y}}_{0:K}^i) + \mathcal{J}_w(\bar{\mathbf{s}}_{0:K}^i, \bar{\mathbf{y}}_{0:K}^i; \mathbf{w}_k^i, \boldsymbol{\alpha}_{w,k}^i), \end{aligned} \quad (1)$$

where \mathcal{J}_g and \mathcal{J}_o are penalty terms for goal reaching and collision avoidance, respectively, which are defined as follows:

$$\begin{aligned} \mathcal{J}_g(\bar{\mathbf{s}}_{0:K}^i) &:= \sum_{\bar{k}=0}^K (\bar{\mathbf{p}}_{\bar{k}}^i - \bar{\mathbf{p}}_g^i)^\top Q_g (\bar{\mathbf{p}}_{\bar{k}}^i - \bar{\mathbf{p}}_g^i), \\ \mathcal{J}_o(\bar{\mathbf{s}}_{0:K}^i, \bar{\mathbf{y}}_{0:K}^i) &:= \sum_{j \in \mathcal{A} \setminus \{i\}} \sum_{\bar{k}=0}^K A_d^2(\bar{\mathbf{s}}_{\bar{k}}^i, \bar{\mathbf{s}}_{\bar{k}}^{j,o}). \end{aligned}$$

Here $Q_g \succ 0$, and A_d denotes the asymmetric Gaussian integral function [23], dependent on the agent's heading. The topology term penalizes deviation from the target winding numbers:

$$\begin{aligned} \mathcal{J}_w(\bar{\mathbf{s}}_{0:K}^i, \bar{\mathbf{y}}_{0:K}^i; \mathbf{w}_k^i, \boldsymbol{\alpha}_{w,k}^i) \\ := \frac{1}{N-1} \sum_{j \in \mathcal{A} \setminus \{i\}} \alpha_{w,k}^{i,j} \left\{ w(\bar{\mathbf{s}}_{0:K}^{i,o}, \bar{\mathbf{s}}_{0:K}^{j,o}) - w_k^{i,j} \right\}^2. \end{aligned} \quad (2)$$

Since we assume policy homogeneity, we also use a common value for the hyperparameters for π^C among agents.

Our main novelty lies in the Planner; the Controller itself follows [8], modified only to incorporate the learned targets \mathbf{w}_k^i and weights $\boldsymbol{\alpha}_{w,k}^i$ via \mathcal{J}_w . The specific design of the MPC algorithm, \mathcal{J}_g and \mathcal{J}_o is not the main part of this work and can be flexibly modified according to the implementation objectives.

4.3 Overall Algorithm

The core idea is to delegate the challenging, symmetry-breaking topological decision to the learning-based Plan-

Algorithm 1 WNumMPC (Winding Number-aware MPC)

Input: $\tilde{K}, \pi_\theta^P, \pi^C$
Output: trajectory of Agent i $\mathbf{s}_{0:k_f}^i$

- 1: $k \leftarrow 0$
- 2: $\tilde{k} \leftarrow \text{Random}(0, \dots, \tilde{K} - 1)$
- 3: **while** not reached goal **do**
- 4: $\mathbf{s}_k^i, \mathbf{y}_k^i \leftarrow \text{getObservation}$
- 5: **if** $k = 0$ or $\tilde{k} \equiv 0 \pmod{\tilde{K}}$ **then**
- 6: $\mathbf{w}_k^i \leftarrow \pi_\theta^P(\mathbf{s}_k^i, \mathbf{y}_k^i)$
- 7: **else**
- 8: $\mathbf{w}_k^i \leftarrow \mathbf{w}_{k-1}^i$
- 9: **end if**
- 10: $\mathbf{u}_k^i \leftarrow \pi^C(\mathbf{s}_k^i, \mathbf{y}_k^i, \mathbf{w}_k^i)$
- 11: $k \leftarrow k + 1, \tilde{k} \leftarrow \tilde{k} + 1$
- 12: **end while**

ner, while the model-based Controller ensures reliable local motion. [Algorithm 1](#) summarizes the procedure. Here, k indexes the MPC time steps; \tilde{k} is an asynchronous counter controlling when agents refresh their winding number plan.

5 Experiments

We evaluated WNumMPC in simulation against ORCA [12], CADRL [3], Vanilla MPC, and T-MPC [8] baselines. Vanilla MPC is the MPC method that does not use winding numbers (i.e., (1) with $\alpha_{w,k}^i = 0$). T-MPC [8] is the MPC method with cost encouraging higher absolute values of winding numbers, without the dynamic weighting (i.e., (1) with $\mathbf{w}_k^{i,j} = 0$ and $\alpha_{w,k}^{i,j} = \text{const.} < 0$). We also conducted real-robot experiments comparing the proposed method with Vanilla MPC and T-MPC to validate effectiveness in the physical world.

5.1 Simulation Experiments

5.1.1 Dynamics

In simulation, agents are holonomic with maximum speed 0.8. The input $\mathbf{u} = (u_x, u_y)$ directly sets the x, y velocity with $\|\mathbf{u}\| \leq 0.8$:

$$f((p_x, p_y, v_x, v_y, \theta, r), (u_x, u_y)) \\ = (p_x + u_x \Delta t, p_y + u_y \Delta t, u_x, u_y, \tan^{-1}(u_y/u_x), r),$$

with control period $\Delta t = 0.1$. All agents have collision radius $r_i = 0.15$.

5.1.2 Instances and Metric

We consider dense scenarios where multiple agents cross simultaneously. Start positions are randomly generated around a circle. More precisely, they are generated by adding random noise to randomly generated positions on the circle. Goals are generated in two ways:

- **Random:** goals are sampled in the same way as the starts.
- **Crossing:** each goal is placed diametrically opposite the start across the circle center.

The circle radius is 2.0 and perturbations are drawn uniformly from $[-0.4, 0.4]$ on each axis. An example of a Crossing instance is shown in [Figure 3](#).

To evaluate methods, we used the *Average Extra Time to Goal*:

$$\bar{t}_e = \frac{1}{n} \sum_{i=1}^N \left[t_g^i - \frac{\|\mathbf{p}_0^i - \mathbf{p}_g^i\|_2}{v_{\max}} \right],$$

a standard metric independent of agent count and start-goal distances [3]. Instances are regarded as a timeout if not all agents reach goals within 20 time units.

5.1.3 Implementation Details

Our implementation is based on [8]. We used Python 3.11 and PyTorch; the Planner is trained with TorchRL [24]. We used the following PPO hyperparameters: a discount factor of 0.95, GAE $\lambda = 0.9$, a clipping threshold of 0.1, and 4 epochs. For scenarios with $N \leq 5$ agents, the learning rate, batch size, and entropy coefficient were set to

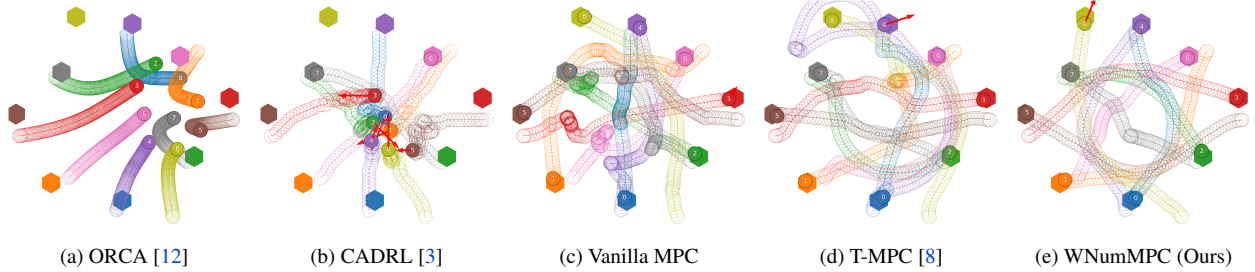


Figure 3: Comparison of agent trajectories in a Crossing scenario, generated by (a) ORCA, (b) CADRL, (c) Vanilla MPC, (d) T-MPC, and (e) WNumMPC. The proposed method (e) efficiently resolves the navigational symmetry, unlike baseline methods that result in deadlocks (a), collisions (b), and inefficient paths (c, d).

4.0×10^{-4} , 1024, and 1.0×10^{-3} , respectively. For scenarios with $N > 5$ agents, these values were adjusted to 2.0×10^{-4} , 4096, and 3.0×10^{-3} , respectively. Unlike [3–5], we train π_θ^P from scratch without behavioral pretraining; the model-based Controller already provides basic navigational competence early in training.

Controller π^C parameters were set as follows: prediction horizon $K = 10$, update period $\bar{K} = 5$ and the shape parameters for A_d , $\sigma_h = 0.5$, $\sigma_r = 0.3$, $\sigma_s = 0.35$. For WNumMPC (our method), T-MPC, and Vanilla MPC, the cost function weights α_g and α_o were tuned for each experimental setup, such as the number of agents, using Optuna [25].

For training of both WNumMPC and CADRL, we used only Random instances. Training was conducted for each number of agents. For CADRL, the model was first pre-trained by imitation on ORCA trajectories for $N = 3$, then tuned with RL for each number of agents. (This recipe was more workable than doing imitation learning for more than three agents.) All baselines are run under the same computational environment with reasonable parameter tuning for fairness.

5.2 Real-World Experiments

We conducted tabletop experiments with differential-drive robots *maru* [9], comparing our method with Vanilla MPC and T-MPC. CADRL and ORCA were omitted due to frequent collisions or timeouts in simulation.

5.2.1 Dynamics

Since *maru* is differential-drive, we adapt the dynamics of agents, which is used in both the Planner’s training and the MPC model. The input $\mathbf{u} = (u_v, \psi)$ denotes linear and angular velocity:

$$\begin{aligned} & f((p_x, p_y, v \cos \theta, v \sin \theta, \theta, r), (u_v, \psi)) \\ &= (p_x + u_v \cos(\theta + \psi \Delta t / 2) \Delta t, \\ & \quad p_y + u_v \sin(\theta + \psi \Delta t / 2) \Delta t, \\ & \quad u_v \cos(\theta + \psi \Delta t), u_v \sin(\theta + \psi \Delta t), \theta + \psi \Delta t, r). \end{aligned}$$

The control interval is $\Delta t = 0.1$ seconds. Inputs satisfy $|u_v + \psi / 7.5| \leq 0.6$ and $|u_v - \psi / 7.5| \leq 0.6$ [9]. Thus, the max linear speed is 0.6 per second in simulator units. The collision radius is $r_i = 0.15$, which corresponds to the physical robot radius 15 mm. We use this value for collision detection in the experiments. On the other hand, to mitigate sim-to-real discrepancies, we use $r_i = 0.20$ in both the training environment and MPC cost computation.

5.2.2 Instances and Metric

We set $N = 7$ and evaluate 100 cases (50 Random + 50 Crossing), alternating them so that goals of one instance serve as starts of the next for continuous operation. The circle radius is 1.5 (about 15 cm), with axis-wise uniform noise in $[-0.3, 0.3]$. The metric is the same as in simulation. The timeout threshold is 30 seconds.

5.2.3 Implementation Details

The Planner policy π_θ^P was trained entirely in a simulation environment using a differential-drive robot model. This policy was subsequently deployed on the physical hardware for zero-shot evaluation, without any fine-tuning or further training on real-world data. All other training configurations and hyperparameters were identical to those used in the simulation.

6 Results

Based on the evaluation metrics of the experimental results, we performed a quantitative analysis of the proposed method and compared its performance with that of existing methods.

6.1 Simulation Results

Figures 4 and 5 (left) report success rate and average extra time to goal across agent counts N and instance types. Conventional methods degraded notably for larger values of N , especially on Crossing instances, whereas WNumMPC maintained high success rates even in dense settings. Moreover, while baselines incurred significantly larger extra time on Crossing, our method kept it low, indicating efficient navigation. These results show that WNumMPC successfully accounts for interactions and breaks symmetry in complex, dynamic environments, with strong scalability in N .

CADRL showed relatively good performance on Random instances except in the densest cases, but its performance degraded even in low-density Crossing instances. This is likely because training was conducted only on Random instances, leading to poor generalization in atypical scenarios. In contrast, our proposed method also trained solely on Random instances, yet still achieved favorable results on Crossing instances. This suggests that the reliability of the MPC component compensates for the shortcomings of purely learning-based approaches.

Figure 3 visualizes trajectories for the same Crossing instance. In ORCA, agents stopped after yielding to each other. In CADRL, agents failed to avoid collisions after gathering in the center. Vanilla MPC successfully avoided collisions, but many agents temporarily stopped. T-MPC

avoided collisions without slowing down, but some agents took extremely long detours. In contrast, WNumMPC successfully avoided collisions efficiently.

Based on the above results, the effectiveness of the proposed method and its superiority over existing methods are demonstrated.

6.2 Real-World Results

Figures 4 and 5 (right) show the real-world results (and, for reference, the corresponding differential-drive simulation).

On Crossing instances, WNumMPC achieved the slightly higher success rate compared to other methods. While vanilla MPC had a smaller average extra time, it is the average only for successful instances. When averaging only the successful instances for both Vanilla MPC and the proposed method, the proposed method yielded a slightly better value (Vanilla MPC: 4.309 s, WNumMPC: 4.301 s). The same holds true when making a similar comparison with T-MPC (T-MPC: 4.59 s, WNumMPC: 4.46 s). This confirms the advantage of our approach in the real world for symmetric scenarios. Compared to the results in simulation, both the existing and proposed methods showed a tendency for performance degradation in real-world experiments in these instances. Our method demonstrated the significantly higher success rate also in simulation, and the performance gap between simulation and real-world was not noticeably larger than other methods. On Random instances, while the success rate of WNumMPC was high in simulation, it was slightly worse in the real-world experiment. In simulations, there was little difference in results among the methods, whereas in real-world scenarios, only the proposed method showed a slight decrease in performance.

The discrepancy between simulation and real-world outcomes can be attributed primarily to the following two factors.

- **Increased timeout rates in Crossing instances:** In real-world settings, delays in communication and actuation make it more difficult for deadlocks to be resolved by chance, unlike in simulations. Consequently, a method without an explicit cooperative strategy, such as Vanilla MPC, suffered the most significant performance degradation.

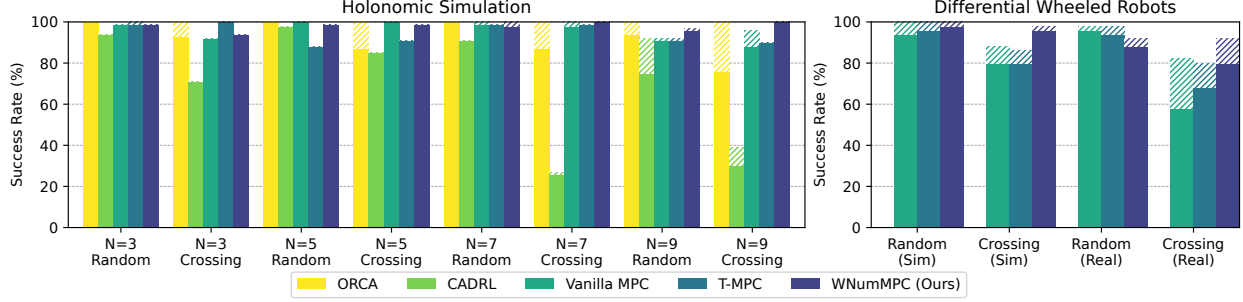


Figure 4: Comparison of Navigation Success Rates (solid bars) and Timeout Rates (hatched bars). (Left) Results in simulations of the holonomic model for each agent count (N) and generation method of instances (Random, Crossing). (Right) Results of the MPC-based methods with $N = 7$ differential wheeled robots in simulations and real-world experiments.

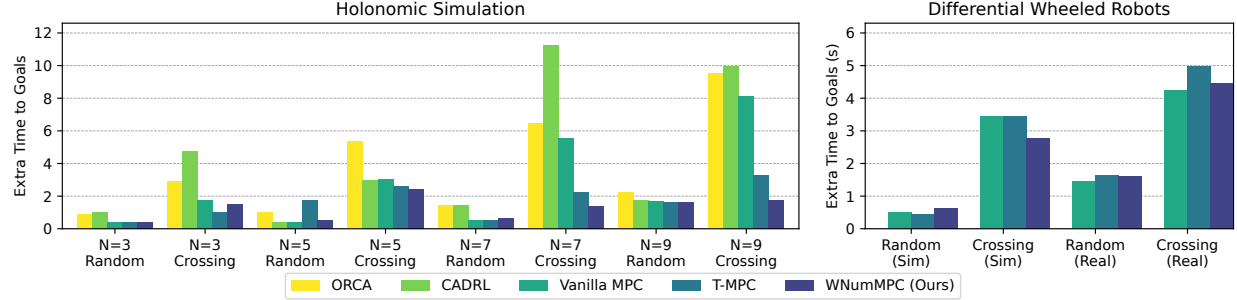


Figure 5: Comparison of Navigation Efficiency Based on Average Extra Time to Goal. (Left) Average extra time in Holonomic model simulations for each agent count (N) and generation method of instances (Random, Crossing). (Right) Average extra time for MPC-based methods with $N = 7$ differential wheeled robots in simulations and real-world experiments.

- **Increased collision rates in the proposed method:** This increase is likely due to the Sim-to-Real gap affecting the learning-based Planner. Since the policy was trained entirely in simulation for zero-shot transfer, it is susceptible to unmodeled physical factors and differences in dynamics. This phenomenon was observed in both types of instances.

These results demonstrate that the learned topological cooperative strategy is effective in the real world, particularly in symmetric situations prone to deadlocks. Notably, the ability to effectively avoid the deadlocks that were the primary cause of performance degradation for existing methods in the Crossing scenario suggests the superi-

ority of our cooperative strategy learning approach in real-world navigation tasks requiring complex interactions and symmetry breaking. On the other hand, it also became apparent that the learning-based Planner is susceptible to the Sim-to-Real gap. Bridging this gap to further enhance the method's reliability will be an important task for future research.

7 Conclusion

In this paper, we propose a novel hierarchical control framework that learns topological cooperative strategies to address a fundamental challenge in decentralized multi-

agent navigation: deadlocks arising from symmetries between agents. This method consists of a learning-based planner that devises topological cooperative strategies and prioritizes coordination among multiple agents, and a model-based controller that generates safe and efficient trajectories based on the plan. Through experiments in both simulation and on real hardware, we demonstrated that the proposed method outperformed existing approaches in terms of both success rate and efficiency, particularly in high-density scenarios. These results suggest that our approach of learning cooperative strategies themselves, rather than relying on fixed rules, is effective for efficiently breaking symmetries between agents and achieving efficient navigation.

As for future work, we envision three directions based on the results of this study. The first is to improve the robustness and generalization of the planner. By incorporating sim-to-real techniques such as Domain Randomization into the planner’s training process, we aim to obtain a highly reliable policy that can bridge the sim-to-real gap. The second direction is to expand the scope of application by advancing the controller. Introducing a state-of-the-art nonlinear model predictive control, such as Model Predictive Path Integral (MPPI), into the controller will enable the application of our framework to agents with more complex dynamics and enhance its control performance. The final direction is to improve the scalability and generality of the framework. By incorporating a Graph Neural Network (GNN) into the planner, we expect to enhance scalability to large-scale agent groups and further enhance the generality of our proposed method.

References

[1] L. Rieger, M. Carlander, N. Lidander, N. Murgovski, and J. Sjöberg, “Centralized mpc for autonomous intersection crossing,” in *2016 IEEE 19th International Conference on Intelligent Transportation Systems (ITSC)*. IEEE Press, 2016, p. 1372–1377.

[2] G. Williams, A. Aldrich, and E. A. Theodorou, “Model predictive path integral control: From theory to parallel computation,” *Journal of Guidance, Control, and Dynamics*, vol. 40, no. 2, pp. 344–357, 2017.

[3] Y. F. Chen, M. Liu, M. Everett, and J. P. How, “Decentralized non-communicating multiagent collision avoidance with deep reinforcement learning,” in *2017 IEEE International Conference on Robotics and Automation (ICRA)*, 2017, pp. 285–292.

[4] M. Everett, Y. F. Chen, and J. P. How, “Motion planning among dynamic, decision-making agents with deep reinforcement learning,” in *2018 IEEE/RSJ International Conference on Intelligent Robots and Systems (IROS)*, 2018, pp. 3052–3059.

[5] Y. F. Chen, M. Everett, M. Liu, and J. P. How, “Socially aware motion planning with deep reinforcement learning,” in *2017 IEEE/RSJ International Conference on Intelligent Robots and Systems (IROS)*, 2017, pp. 1343–1350.

[6] F. Feurtey, “Simulating the collision avoidance behavior of pedestrians,” Master’s thesis, University of Tokyo, 2000.

[7] C. Mavrogiannis and R. A. Knepper, “Hamiltonian coordination primitives for decentralized multiagent navigation,” *The International Journal of Robotics Research*, vol. 40, no. 10-11, pp. 1234–1254, 2021.

[8] C. Mavrogiannis, K. Balasubramanian, S. Poddar, A. Gandra, and S. S. Srinivasa, “Winding through: Crowd navigation via topological invariance,” *IEEE Robotics and Automation Letters*, vol. 8, no. 1, pp. 121–128, 2023.

[9] S. Ichihashi, S. Kuroki, M. Nishimura, K. Kasaura, T. Hiraki, K. Tanaka, and S. Yoshida, “Swarm body: Embodied swarm robots,” in *Proceedings of the 2024 CHI Conference on Human Factors in Computing Systems*, ser. CHI ’24. New York, NY, USA: Association for Computing Machinery, 2024.

[10] G. Ferrer, A. Garrell, and A. Sanfeliu, “Social-aware robot navigation in urban environments,” in *2013 European Conference on Mobile Robots*, 2013, pp. 331–336.

[11] J. van den Berg, M. Lin, and D. Manocha, “Reciprocal velocity obstacles for real-time multi-agent navigation,” in *2008 IEEE International Conference on Robotics and Automation*, 2008, pp. 1928–1935.

[12] J. van den Berg, S. J. Guy, M. Lin, and D. Manocha, “Reciprocal n-body collision avoidance,” in *Robotics Research*, C. Pradalier, R. Siegwart, and G. Hirzinger, Eds. Berlin, Heidelberg: Springer Berlin Heidelberg, 2011, pp. 3–19.

[13] L. Streichenberg, E. Trevisan, J. J. Chung, R. Siegwart, and J. Alonso-Mora, “Multi-agent path integral control for interaction-aware motion planning in urban canals,” in *2023 IEEE International Conference on Robotics and Automation (ICRA)*, 2023, pp. 1379–1385.

[14] S. Liu, P. Chang, W. Liang, N. Chakraborty, and K. Driggs-Campbell, “Decentralized structural-rnn for robot crowd navigation with deep reinforcement learning,” in *2021 IEEE International Conference on Robotics and Automation (ICRA)*, 2021, pp. 3517–3524.

[15] M. Berger, “Topological invariants in braid theory,” *Letters in Mathematical Physics*, vol. 55, pp. 181–192, 01 2001.

[16] C. I. Mavrogiannis and R. A. Knepper, “Multi-agent path topology in support of socially competent navigation planning,” *The International Journal of Robotics Research*, vol. 38, no. 2-3, pp. 338–356, 2019.

[17] C. Mavrogiannis, J. A. DeCastro, and S. Srinivas, “Implicit multiagent coordination at uncontrolled intersections via topological braids,” in *International Workshop on the Algorithmic Foundations of Robotics*. Springer, 2022, pp. 368–384.

[18] C. Cao, P. Trautman, and S. Iba, “Dynamic channel: A planning framework for crowd navigation,” in *2019 international conference on robotics and automation (ICRA)*. IEEE, 2019, pp. 5551–5557.

[19] M. Kuderer, C. Sprunk, H. Kretzschmar, and W. Burgard, “Online generation of homotopically distinct navigation paths,” in *2014 IEEE International Conference on Robotics and Automation (ICRA)*. IEEE, 2014, pp. 6462–6467.

[20] D. Martinez-Baselga, O. de Groot, L. Knoedler, L. Riazuelo, J. Alonso-Mora, and L. Montano, “Shine: Social homology identification for navigation in crowded environments,” *The International Journal of Robotics Research*, p. 02783649251344639, 2024.

[21] J. Schulman, F. Wolski, P. Dhariwal, A. Radford, and O. Klimov, “Proximal policy optimization algorithms,” *ArXiv*, vol. abs/1707.06347, 2017.

[22] E. F. Camacho and C. B. Alba, *Model Predictive Control*, 2nd ed., ser. Advanced Textbooks in Control and Signal Processing. London, England: Springer, May 2004.

[23] R. Kirby, “Social robot navigation,” Ph.D. dissertation, Carnegie Mellon University, Pittsburgh, PA, May 2010.

[24] A. Bou, M. Bettini, S. Dittert, V. Kumar, S. Sodhani, X. Yang, G. D. Fabritiis, and V. Moens, “Torchrl: A data-driven decision-making library for pytorch,” 2023.

[25] T. Akiba, S. Sano, T. Yanase, T. Ohta, and M. Koyama, “Optuna: A next-generation hyperparameter optimization framework,” in *Proceedings of the 25th ACM SIGKDD International Conference on Knowledge Discovery and Data Mining*, 2019.